1.D.1 *Nuclear Physics* **89** (1966) 673—685;

DEFORMATIONS IN THE CALCIUM REGION

GEORGE F. BERTSCH †
Palmer Physical Laboratory, Princeton, New Jersey ††

Received 9 May 1966

Abstract: A deformed model is applied to the excited states of the nuclei ^{40}Ca, ^{42}Ca and ^{41}Ca. The deformed states are based on two-particle, two-hole, Nilsson wave functions and have admixtures of the shell-model states induced by a two-body force. The electromagnetic matrix elements, stripping and pick-up reactions and energy systematics are compared with experiment. Agreement is reasonable for ^{40}Ca, but there is disagreement and possibly inconsistency of the model with experiment in ^{42}Ca.

1. Introduction

Many experimental data have recently been accumulated on the properties of excited states of nuclei near the doubly-magic ^{40}Ca. Very few states are allowed by the simple shell model based on a closed ^{40}Ca core, but in fact many states are observed at low energy (less than 4 MeV excitation). As general features, these extra states have quadrupole strengths and spectra characteristic of permanently deformed nuclei, as well as a propensity to mix strongly with the shell-model states. An example which has been emphasized by Bohr and Mottelson is the first excited 0^+ state in ^{42}Ca, which has a B(E2) strength to the first 2^+ state of 600 e^2fm^4, as compared with the single-particle estimate of 40 e^2fm^4.

States with these remarkable properties are also observed in the oxygen region, where they are even more striking †††. For this region, a microscopic theory has been developed, which in several respects is quite successful [1–8]). One considers the low-lying excitations of natural parity to be deformed states, based on a shell-model wave function with two or more single-particle excitations. The idea that excitations of spherical nuclei may be deformed originated with Morinaga [1]) and the first convincing calculations were carried out by Brink and Nash [2]), who showed that the lowest, two-particle-two-hole states should be the states of maximum prolate deformation, i.e. with the valence particles along some intrinsic polar axis, and the valence holes in the median plane. Unfortunately, the calculated excitation energy of these states, both 2p-2h and 4p-4h, is at least 13 MeV above what is required by the experimental positions of the extra states [4, 5]). However, ignoring this disturbing point, Engeland

† National Science Foundation Post-Doctoral Fellow.
†† Visitor at the Niels Bohr Institute, Copenhagen, 1965–66.
††† References to the oxygen experimental data are in ref. [3]).

investigated the mixing between the two-particle excitations and the shell-model states [6]). Brown found that this mixing could account for the many large $B(E2)$ strengths in the oxygen region [7]). Investigating the mixing to be expected from realistic forces [3]), satisfactory agreement was found for ^{16}O, but the experimental mixing was somewhat larger than the theoretical expectation for ^{18}O. As will be seen, a similar situation occurs in the calcium region.

We shall develop the corresponding theory for the calcium region along the same lines and compare with experiment. We first discuss the form of the wave functions, then the calculation of the mixing and finally the properties of the states obtained.

2. The Wave Function

The deformed wave function is assumed to have two particles lifted from the s-d shell to the f-p shell. One could also consider 4p-4h components in the wave function, as Brown and Green [3]) did, but there is not yet sufficient information on higher excited states in calcium to confirm the mixing between different deformed bands or to specify their eigenenergies.

Even considering just two-particle excitations, the valence wave functions are too complicated to be determined by diagonalizing a shell-model Hamiltonian. Instead, the valence particles will be coupled together with the aligned coupling scheme [43]), according to which, the particles are in independent single-particle orbitals which maximize the quadrupole deformation along some intrinsic axis. States of definite angular momentum may be projected out of the intrinsic wave function by a Hill-Wheeler integral.

We have some confidence that this procedure will produce states close to the eigenvectors of some realistic shell-model Hamiltonian. This is based partly on the experience in the oxygen region, where both configuration mixing calculations [4, 17]) and the simpler Hartree-Fock calculations have shown that the deformed wave functions are quite good even with realistic forces. In the calcium region, there have been matrix diagonalization calculations with configurations limited to the $f_{\frac{7}{2}}$ shell [15]) †, which produce eigenvectors remarkably close to the $f_{\frac{7}{2}}$ wave functions of the aligned coupling scheme [18]).

The SU(3) classification of states [9, 10]) provides a simple and elegant method for defining intrinsic deformed states and projecting out definite angular momentum, when there is maximal spacial symmetry in the wave function. Where the spin-orbit force competes effectively with the deformed field, as in calcium, the space symmetry becomes complicated, and it is easier to define the single-particle orbitals in a spherical basis rather than the Cartesian basis of SU(3).

The particular mixture of spherical states in a deformed orbital was determined by

† It has also been found by Bayman [44]) that a matrix diagonalization for the lowest 3p–1h state in ^{48}Sc yields a wavefunction in the $(f_{\frac{7}{2}})^4(d_{\frac{3}{2}})$ configuration practically identical to the aligned coupling wave function.

Nilsson [11]) as a function of the deformed field. We shall use these orbitals in the intrinsic wave function. The intrinsic wave function may now be written as the product

$$\psi_{\mathrm{def}}^{\mathrm{int}}(^{40}\mathrm{Ca}) = \{\tilde{f}_{\frac{7}{2},\frac{1}{2}}\tilde{f}_{\frac{7}{2},-\frac{1}{2}}\tilde{d}^{-1}_{\frac{3}{2},\frac{3}{2}}\tilde{d}^{-1}_{\frac{3}{2},-\frac{3}{2}}\}\phi_{\mathrm{core}}, \tag{1a}$$

$$\psi_{\mathrm{def}}^{\mathrm{int}}(^{41}\mathrm{Ca}) = \tilde{f}_{\frac{7}{2},\frac{1}{2}}\psi_{\mathrm{def}}^{\mathrm{int}}(^{40}\mathrm{Ca}), \tag{1b}$$

$$\psi_{\mathrm{def}}^{\mathrm{int}}(^{42}\mathrm{Ca}) = \tilde{f}_{\frac{7}{2},\frac{1}{2}}\tilde{f}_{\frac{7}{2},-\frac{1}{2}}\psi_{\mathrm{def}}^{\mathrm{int}}(^{40}\mathrm{Ca}). \tag{1c}$$

The particular orbitals chosen, $\tilde{f}_{\frac{7}{2},\frac{1}{2}}$ (Nilsson no. 14) and $\tilde{d}_{\frac{3}{2},\frac{3}{2}}$ (Nilsson no. 8) give the most favourable two-particle excitation in energy when the deformation is prolate. It should be noted that this definition of the wave function differs from the SU(3) prescription even in the limit that the spin can be neglected. The SU(3) representation [6, 4] ,which is the appropriate one for ^{40}Ca, has equal mixture of s- and d-holes, whereas the no. 8 Nilsson orbital has no s-amplitude.

The wave function is still not completely specified because the permutation symmetry is not uniquely determined. We first consider the isospin coupling scheme that gives the maximum spacial symmetry in the limit that the spin-orbit splitting is small or that the deformation is large. (This is the SU(3) limit and Nilsson's $\eta \gg 1$ limit.) Then the wave functions are

$$^{40}\mathrm{Ca} = \sqrt{\tfrac{1}{2}}[(\mathrm{pp})^{T=1}(\mathrm{hh})^{T=1}]^0 + \sqrt{\tfrac{1}{2}}[(\mathrm{pp})^{T=0}(\mathrm{hh})^{T=0}]^0, \tag{2a}$$

$$^{41}\mathrm{Ca} = \sqrt{\tfrac{1}{2}}[(\mathrm{ppp})^{\frac{1}{2}}(\mathrm{hh})^1]^{\frac{1}{2}} + \sqrt{\tfrac{1}{2}}[(\mathrm{ppp})^{\frac{1}{2}}(\mathrm{hh})^0]^{\frac{1}{2}}, \tag{2b}$$

$$\mathrm{Ca}^{42} = (\mathrm{p}^4)^0(\mathrm{hh})^1. \tag{2c}$$

The force mixing states of different internal isospin structure may be small in comparison to the separation of the unperturbed states. The mixtures given by the wave functions (2) are therefore not reliable, and we also consider the scheme with the two holes always coupled to $T = 1$,

$$^{40}\mathrm{Ca} = [(\mathrm{pp})^1(\mathrm{hh})^1]^0, \text{ etc.} \tag{2d}$$

This scheme would certainly be better for heavy nuclei, where pairing is important. Also it is more in agreement with a rule proposed by Zamick [12]) that maximum T of the particles be coupled to maximum T of the holes.

Before physical states of definite angular momentum can be projected out of the intrinsic wave functions, we have to know the behaviour of the deformed core ϕ_{core} under rotations. For axially symmetric cores, the expansion can be made in angular momentum eigenstates,

$$\phi_{\mathrm{core}} = \sum_{L\,\mathrm{even}} a_L\{\phi_{\mathrm{core}}\}^L_{M=0}. \tag{3}$$

From calculations in perturbation theory [13]) it is known that the core behaves much like a Nilsson product wave function. Then it is reasonable to calculate the coefficients a_n from formulae (2.34) and (2.40) of Arima and Yoshida [14]) which are valid for pure quadrupole deformations.

In principle there will be a different core deformation for each of the nuclei ^{40}Ca, ^{41}Ca and ^{42}Ca. However, to a good approximation the deformation is linear in the number of valence particles. The extra valence particles in ^{41}Ca and ^{42}Ca have an equal polarizing effect in the "spherical" and "deformed" configurations, and so do not contribute to the overlap

$$\langle \phi_{\text{core}}^{\text{def}} | \phi_{\text{core}}^{\text{sph}} \rangle .$$

Thus their effect may be neglected in eq. (3) for calculating the mixing between deformed and spherical states.

For the small deformations which are indicated by perturbation theory, only $L = 0$ and $L = 2$ contribute significantly to the core wave function, and it is sufficient to know a_0 given by

$$a_0 \approx \langle \phi_{\text{core}}^{\text{def}} | \phi_{\text{core}}^{\text{sph}} \rangle . \tag{4}$$

States of definite angular momentum are now projected out of the intrinsic wave function. First the Nilsson orbitals are expressed in terms of spherical orbitals, and then pairs of wave functions are combined according to

$$\{ \phi_{m_1}^{j_1} \phi_{m_2}^{j_2} \} = \sum_J \langle j_1 \, j_2 \, m_1 \, m_2 | JM \rangle \{ \phi^{j_1} \phi^{j_2} \}^J ,$$

until the intrinsic wave function is expressed as a sum over wave functions with definite total J (ref. [18])). For the wave functions considered here, where there are at most two particles of a kind in a given orbital, antisymmetry of the wave function requires only that identical particles in the same orbit be coupled to even J:

$$A(jmj-m) = \sum_{J \text{ even}} \sqrt{2} (jjm \; -m | J0 \rangle (jj)^J .$$

With more than two particles in an orbital, as for example in ^{43}Ca, more advanced techniques are required for projection.

3. Mixing of Deformed and Shell-Model States

In defining the states above we have presumably accounted for all of the particle-particle interaction except for the scattering off-diagonal in the orbitals of both particles. The most important effect of this interaction will be to mix the two types of states with the matrix element,

$$\langle {}^{40+n}\text{Ca}_{\text{spher}}(L) | V | {}^{40+n}\text{Ca}_{\text{def}}(L) \rangle = \sum_J \alpha_J \langle | V | \{ (\tilde{\text{f}}\tilde{\text{f}})^J (\text{d}^{-1}\text{d}^{-1})^J \}^0 \rangle \times \langle (\tilde{\text{f}}^n)^L | \psi_{\text{shell model}}(L) \rangle \langle (\phi_{\text{core}}^{\text{def}})^{L'} | \phi_{\text{core}}^{\text{sph}} \rangle , \tag{5}$$

where the coefficients α_J are the expansion coefficients of

$$| \{ (\tilde{\text{f}}\tilde{\text{f}})^J (\text{d}^{-1}\text{d}^{-1})^J \}^0 \{ (\tilde{\text{f}}^n)^L (\phi_{\text{core}}^{\text{def}})^{L'} \}^L \rangle$$

in the projected deformed wave function.

It is useful to consider two limiting situations, i.e. with small core deformation and with very large core deformation. When the core can be neglected, V may be computed from the intrinsic valence wave function as follows:

$$\langle|V|\psi_{int}(\text{2p-2h})\rangle = \langle|V|\sum_L c_L\psi^L(\text{2p-2h})\rangle = c_0\langle|V|\psi^0(\text{2p-2h})\rangle. \tag{6}$$

The result is that the physical matrix element is enhanced over the intrinsic matrix element by the factor $1/c_0$, where the c-coefficients may be expressed analytically in the SU(3) limit [9]).

In the opposite extreme of large core deformations ($\beta \geqq 0.4$ for Ca), it is reasonable to describe the core by

$$\langle\phi^{\text{def}}_{\text{core}}(\Omega)|\phi^{\text{def}}_{\text{core}}(\Omega')\rangle \approx \delta(\Omega-\Omega'). \tag{7}$$

This implies for the angular momentum decomposition,

$$\phi^{\text{def}}_{\text{core}} \approx a_0\sum_L \phi^{L,0}_{\text{core}}\sqrt{2L+1} \qquad \text{for low } L. \tag{8}$$

Using this in eq. (5), the physical matrix element becomes

$$\langle|V|[\psi\phi]^0\rangle = a_0\langle|V|\psi_{\text{int}}(\text{2p-2h})\rangle. \tag{9}$$

The previous enhancement is replaced by a hindrance due to the imperfect overlap of the undeformed and deformed cores. At the deformations of interest, neither of these approximations is valid and the projection must be done explicitly.

The only component of the force that contributes to the matrix element in the SU(3) limit is the central even force of highest possible relative momentum,

$$\langle|V|\psi_{\text{int}}([6,4])\rangle = \frac{\sqrt{2}}{\sqrt{3}\cdot 16(\frac{9}{7}+\frac{2}{3}+\frac{9}{11})^{\frac{1}{2}}}\left(\frac{3}{\sqrt{7}}\langle\text{2S}||V||\text{3S}\rangle+\tfrac{10}{7}\sqrt{6}\langle\text{1D}||V||\text{2D}\rangle\right). \tag{10}$$

Here the notation is with harmonic oscillator wave functions, and $|NL\rangle$ represents the relative wave function of angular momentum L and N nodes. For these matrix elements, a useful realistic interaction is the one defined by Kallio and Kolltveit [19]), which is the long range part of an S-state force with a hard core. This interaction has been quite successful for calculating Hartree-Fock energies and two-particle spectra, but it predicts too low a nuclear radius. In this calculation a constant separation distance is used, which may mean that the high momentum components are overestimated by 30–50 % (refs. [20, 21])). In fig. 1 the physical matrix element is plotted for ^{40}Ca and ^{42}Ca as a function of deformation of core and valence orbitals, and assuming form (2d) for the ^{40}Ca wave function. Here the deformation parameter is

$$\beta = \tfrac{4}{3}\sqrt{\tfrac{1}{5}\pi}\delta \tag{11}$$

in terms of Nilsson's deformation parameter δ.

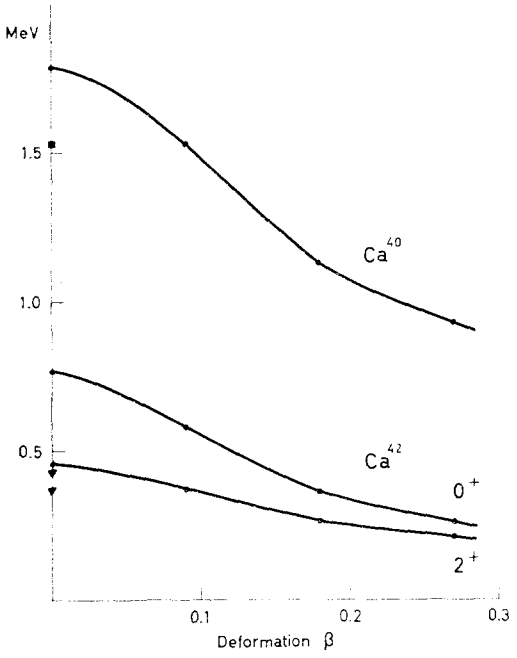

Fig. 1. The matrix element mixing deformed and shell-model states is shown as a function of deformation of core and valence particles. The matrix element in the [6, 4] SU(3) representation of ^{40}Ca and the spin 0^+, 2^+ states of the [12, 4] SU(3) state of ^{42}Ca are indicated by a square and triangles, respectively.

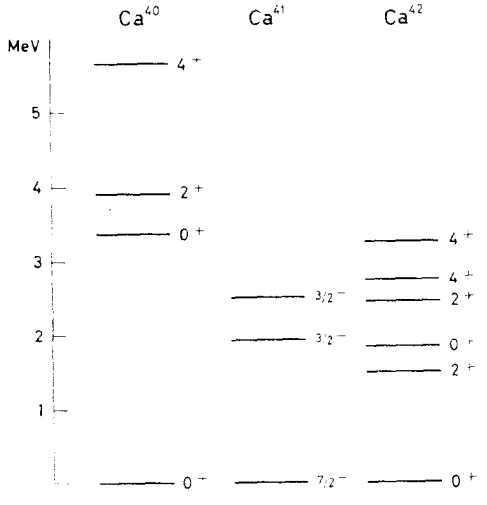

Fig. 2. Calcium spectra. The positions of levels discussed in the text are shown above, taken from refs. [22–25]) for ^{40}Ca, ^{41}Ca, ^{42}Ca and the highest 4^+ in ^{42}Ca, respectively.

Two effects make the ^{40}Ca matrix element so much larger than the ^{42}Ca matrix element. The overlap of the extra valence particles contributes a factor 2, and the coherence of different spin and isospin states from (2) provides a factor $\approx \sqrt{6}$ or $\sqrt{3}$ enhancement in the ^{40}Ca matrix element over the ^{42}Ca matrix element, depending on the isospin assumption for the deformed ^{40}Ca. In ^{42}Ca, the shell-model states of lower spin mix more strongly than the higher spins because the orientation of the intrinsic axis is more restricted in the latter case.

In accordance with the discussion in sect. 2, we assume in the further calculation $\beta = 0.17$ with a core overlap

$$\langle \phi^{\mathrm{def}}_{\mathrm{core}} | \phi^{\mathrm{sph}}_{\mathrm{core}} \rangle^2 = 0.78.$$

However, it may be seen from the figure that the value of the matrix element is rather insensitive to the choice of β.

Fig. 2 shows the relevant part of the spectra of the calcium isotopes. Knowing the physical separation of the states E and the mixing force V, the mixing amplitude and level shift are given simply as

$$\mathrm{tg}\,\theta = \frac{E}{2V} - \sqrt{\left(\frac{E}{2V}\right)^2 - 1}, \tag{12a}$$

$$\Delta E = \tfrac{1}{2}E - \sqrt{(\tfrac{1}{2}E)^2 - V^2}. \tag{12b}$$

Table 1 gives the computed mixing angle for the various states considered. It may be seen that the first isospin assumption is inconsistent with the physical positions of the ^{40}Ca and ^{41}Ca states. In the calculation of properties of states that follows, we shall use the mixing computed with the second assumption for ^{40}Ca and assume strongest possible mixing for ^{41}Ca($\frac{3}{2}^-$).

TABLE 1

Theoretical mixing between deformed and spherical Ca states

States	Physical separation (MeV)	V_{KK}	tg θ
^{40}Ca $(0^+)_{\mathrm{I}}$	3.35	1.61	≈ 1
^{40}Ca $(0^+)_{\mathrm{II}}$		1.136	0.396
^{41}Ca $(\frac{3}{2}^-)_{\mathrm{I}}$	0.522	0.63	too strong
^{41}Ca $(\frac{3}{2}^-)_{\mathrm{II}}$		0.52	too strong
^{41}Sc $(\frac{3}{2}^-)$	0.71		0.436 [a])
^{42}Ca (0^+)	1.836	0.359	0.204
^{42}Ca (2^+)	0.900	0.276	0.342
^{42}Ca (4^+)	0.501	0.243	≈ 1

The wave function of the more bound state is given by

$$\psi = \cos\theta|\psi \text{ shell-model}\rangle + \sin\theta|\psi \text{ deformed}\rangle.$$

For ^{40}Ca and ^{41}Ca, the mixing is given for the two isospin assumptions.

[a]) This is assuming maximum mixing in ^{41}Ca, and that the mixing force is independent of T_z.

One case where the level shift is possibly observable † is in ^{40}Ca, where a rotational band defines the unperturbed 0^+ position by the rule

$$E = E_0 + AJ(J+1). \tag{13}$$

Defining the band parameters by the 2^+ and 4^+ states, this results in $\Delta E_{\text{theor.}} = 0.5$ MeV as compared to $\Delta E_{\text{exp}} = 0.2$ MeV. Unfortunately, the 6^+ state is also perturbed by mixing with another band, so there is no independent check on the $J(J+1)$ rule.

4. Physical Properties of States

The wave functions which have been constructed are best tested by evaluating electromagnetic transition operators. Because the core plays an important role in the E2 and E0 matrix elements, the core wave functions of perturbation theory were used explicitly in evaluating these operators. For the E2 operator, the results are nearly the same as simply assuming an effective charge $e = 0.5$ for the valence particles [27]††, as may be seen from table 2.

TABLE 2

Quadrupole moment of deformed and shell-model configurations

State	Valence contribution	Core	Total	Eff. charge
^{40}Ca	7 ν^{-1}	5.9	12.9	12
^{41}Ca	11.6	5.2	16.8	22.2
^{41}Sc	7.3	8.9	16.2	22.3
^{42}Ca	14.0	8.7	22.7	30
neutron $f_{\frac{7}{2}} \rightarrow f_{\frac{7}{2}}$	0	1.42	1.42	1.07
neutron $p_{\frac{3}{2}} \rightarrow f_{\frac{7}{2}}$	0	1.23	1.23	1.36
proton $p_{\frac{3}{2}} \rightarrow f_{\frac{7}{2}}$	2.72	0.44	3.16	4.08

Expectation of the quadrupole operator $Q = 2z^2 - x^2 - y^2$ is taken in states with $L_z = 0$. The values in the last column are assuming effective charges $e_n = 0.5$, $e_p = 1.5$ and SU(3) wavefunctions for the deformed states. Units are the harmonic oscillator parameter $\nu = M\omega/\hbar$.

The deformed wave functions are too complicated to evaluate the E2 operator in the angular momentum eigenstates. Instead, the matrix element is found in the intrinsic frame, and this is multiplied by a projection factor

$$B(ML : I_i \rightarrow I_f) = P\langle\psi_{\text{int}}||\mathrm{M}||\psi_{\text{int}}\rangle.$$

The deformed Nilsson wave functions are quite similar to SU(3) wave functions, so the SU(3) projection factor [9]

$$P = \left(\frac{2I_f+1}{2I_i+1}\right)^2 (I_f 200|I_i 0)^2 \frac{C^2(0, I_i)}{C^2(0, I_f)}, \qquad I_i < I_f$$

† It has been suggested that [16]) the ^{42}Ca(2^+) level shift is also observable by comparing with the ^{50}Ti spectrum.

†† An effective charge of this magnitude was found by Zamick for the $f_{\frac{7}{2}}$ shell.

may be used with little error [3]). Another approximation, which gives results smaller by only 20 %, is to assume that the total wave function has a large deformation in the sense of eqs. (7) and (8). The projection factor then reduces to the well-known [26])

$$P = (I_f 200 | I_i 0)^2.$$

Transitions between physical states can take place via deformed-to-deformed matrix elements, shell-model-to-shell-model matrix elements or a crossover deformed-to-shell-model matrix element. The last possibility may be thought of as a perturbation, with a one-hole intermediate state connected to the shell-model state by an electromagnetic interaction and to the two-hole deformed state by a potential interaction. A simple estimate in perturbation theory indicates that this matrix element should be quite small, less than 1 % of the total matrix element. The absence of 2γ monopole decay in competition with pair production is further evidence that this matrix element is negligible [28]). Table 3 shows the theoretical B(E2) values calculated as described above, compared with experimental values. Harmonic oscillator wave functions have been used with $M\omega/\hbar = \nu = 0.27$ fm^{-2}.

TABLE 3

Theoretical B(E2) in the Ca region compared with experiment

Transition	Theory ($e^2 \cdot$ fm^4)	Experiment
^{40}Ca $(2^+ \rightarrow 0^+)$	13	29 [a])
^{41}Ca $(\frac{3}{2} \rightarrow \frac{7}{2})$	15	129 [b])
^{41}Sc $(\frac{3}{2} \rightarrow \frac{7}{2}^-)$	68	153 [b])
^{42}Ca $(2_1^+ \rightarrow 0_1^+)$	14	72 [c])
^{42}Ca $(0_2^+ \rightarrow 2_1^+)$	76	600 [d])

[a]) Ref. [29]).
[b]) Ref. [30]).
[c]) Ref. [32]).
[d]) Ref. [33]).

There is disagreement for ^{41}Ca and ^{42}Ca. In the ^{41}Ca-^{41}Sc pair †, the near equality of the B(E2) is an indication that the ground state has a large deformed component, because, as may be seen from table 2, the deformed wave functions have nearly equal quadrupole moments, whereas the shell-model wave functions have quite different Q. This effect will go even further in the $A = 42$ nuclei, where ^{42}Sc should have smaller electric matrix elements than ^{42}Ca. This is because the deformed state of ^{42}Sc has some of the proton holes replaced by neutron holes, which do not contribute to E2 and E0 matrix elements when core effects are neglected.

Monopole transitions have been observed [31, 34]) in both ^{40}Ca and ^{42}Ca. The theoretical monopole matrix element, which is essentially the difference of the r^2 charge distribution for the deformed and shell-model states [36]), receives a significant contribution from both the valence wave function and core wave function [13]). The computed

† The author thanks J. Damgaard for bringing this datum to his attention.

value of the operator $M = \sum r_p^2$ is given in table 4 and compared with experiment. Again there is a large discrepancy for ^{42}Ca, indicating much more mixing in ^{42}Ca than we have accounted for [35]). This discrepancy persists even when maximum mixing is allowed for the 0^+ wave functions.

TABLE 4
Monopole transition matrix elements in Ca

Transition	Theory (fm^2)	Experiment
^{40}Ca $(0^+ \to 0^-)$	2.5	2.56 [a])
^{42}Ca $(0^+ \to 0^+)$	1.9	7.00 [b])

[a]) Ref. [31]). [b]) Ref. [34]).

One measurement that is independent of the mixing is the E2/M1 branching ratio of the ^{42}Ca$(2_2^+ \to 2_2^+)$ transition. When the M1 is calculated with the simplified Nilsson wave function of Lawson [18]), the ratio is E2/M1 = 0.12, which may only be compared to the experimental limit E2/M1 < |0.2| of Mitchell [45]). Using this value of the M1 width, we find a branching ratio of the two transitions

$$\Gamma(2_2^+ \to 2_1^+)/\Gamma(2_2^+ \to 0_1^+) = 2.3,$$

as compared to the experimental value

$$\Gamma(2_2^+ \to 2_1^+)/\Gamma(2_2^+ \to 0_1^+) = 3,$$

as measured by Mitchell [†].

Experimental information is also available from stripping and pick-up reactions among various nuclei in the $f_{\frac{7}{2}}$ shell. Nuclear structure information may be extracted only if the Born approximation can be used, which is the case for one-body transfer, but may not be for such complicated reactions as (t, p). Assuming the validity of DWBA or PWBA, the ratio of cross sections to states of the same spin is given directly by the spectroscopic factors, except for an unimportant kinematic factor. The spectroscopic factors are proportional to the overlaps

$$\langle \psi^{n+1}(L) | [a_f^+ \psi^n(L')]^L \rangle, \qquad \langle \psi^{n+2}(L) | [(a_f^+ a_f^+)^L \psi^n(L')]^L \rangle,$$

which are easily found once the projection of the deformed intrinsic states has been done. The theoretical and experimental ratio of cross sections is given in table 5. In calculating the spectroscopic factors from ^{43}Ca, the $\frac{7}{2}^-$ ground state was assumed to be pure shell model. Since the deformed states of ^{43}Ca should follow the band spectrum with $K = \frac{3}{2}$, the $\frac{7}{2}^-$ deformed state may be high enough in energy so that the mixing with the shell-model state can be neglected.

[†] This is also consistent with measurements of McCullen and Haight [43]).

TABLE 5

Ratio of cross sections in pick-up and stripping reactions to final states of the same spin

Reaction	Spin	Theory	Experiment
^{40}Ca(d, p)^{41}Ca	$\frac{3}{2}$	0.4	0.34 [a]
^{40}Ca(^{3}He, d)^{41}Sc	$\frac{3}{2}$	0.04	0.1 [b]
^{40}Ca(t, p)^{42}Ca	0	0.00	0.1 [c]
	2	0.15	0.3
	4	0.4	0.14
^{43}Ca(d, t)^{42}Ca	2	0.12	1 [d]

[a]) Ref. [23]).
[b]) Ref. [38]).
[c]) Refs. [41, 25]).
[d]) Ref. [42]).

One final reaction measurement is the probability of finding an $f_{\frac{7}{2}}$ neutron in the ground state of ^{40}Ca (refs. [37, 38])). This is at least of the order 0.14–0.28, to be compared with 0.13 from the theory.

5. Energy Systematics

If the wave functions which have been calculated are to be believed, it should be possible to understand the systematics of the excitation energies. The absolute position of the deformed states is not understood and furthermore there does not seem to be much hope of calculating it, as it is the difference of two large numbers – the unperturbed energy of a two-particle-two-hole excitation and the energy gained by some strong, as yet unexplained, configuration mixing.

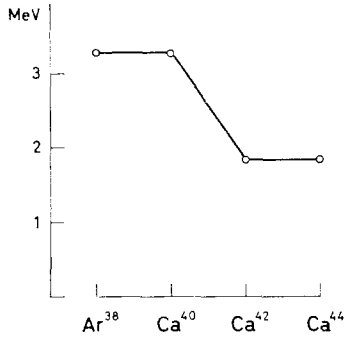

Fig. 3. Systematics of the excitation energy of the first 0^+ excitation in doubly even nuclei near ^{40}Ca. The ^{38}Ar state was observed by Whitten [46]).

However, we may accept the unperturbed position of the 2p-2h configuration as a parameter and just try to calculate the variation of the excitation energy of the deformed state among adjacent nuclei. The changes of excitation energy due to the addition of more valence particles receive contribution from (i) the change of the shell-

model single-particle energy of these particles in the deformed configuration, (ii) the interaction of the valence particles with the 2p-2h configuration, and (iii) the interaction of the extra valence particles with the core deformation. Using SU(3) deformed wave functions and the Kallio-Kolltveit force, these energy changes for the ^{40}Ca-^{42}Ca pair are

$$\Delta E_1 + \Delta E_2 + \Delta E_3 = 5.4 - 4.9 - 5.4 = -4.9 \text{ MeV}.$$

Thus the ^{40}Ca deformed state shouls lie about 5 MeV higher than the deformed state in the neighbouring nuclei. This behaviour is due to the well-known fact that deformed states gain energy with the addition of more valence particles more rapidly than spherical states. The empirical systematics (see fig. 3), show no such jump but rather suggest the smoothness of the vibrational [40]) or core excitation [39]) model. Of course, if there were a large amplitude of 4p-4h excitation in the first excited ^{40}Ca state, as was found to be necessary in ^{16}O to explain the experimental data [3]), the simple argument on energy systematics would be invalidated. A detailed calculation of the moment-of-inertia parameter for the rotational band might help distinguish at least, whether the first excited ^{40}Ca state is based principally on 2p-2h or 4p-4h.

6. Conclusion

The discrepancy between the calculated transition properties and experiment is so large for ^{42}Ca, that we would like to consider the possibility of stronger mixing than the realistic forces allow. In general, further corrections to the wave function, in the form of adding more configurations to the wave function, go in the direction of making the two basic wave functions more dissimilar and thus allow less mixing. On the other hand, a radical change in the isospin part of the wave function, away from the guiding principle of supermultiplet symmetry [12]), would make the core excitation more independent of the extra valence particles and thus could allow stronger mixing. However, it is difficult to see how the 0^+ and 2^+ could be mixed stronger without having a correspondingly large mixing matrix element for the 4^+ states.

A stronger mixing of the 0^+ and 2^+ would make the energy perturbation ΔE significant, opening the interesting possibility that the unperturbed position of the deformed 2^+ be lower than that of the spherical 2^+. This would allow the deformed 0^+, 2^+, 4^+ to be placed in a band satisfying eq. (13). Qualitative agreement with experiment could then also be made with all of the transition matrix elements except the electric monopole.

The author is greatly indebted to G. E. Brown, who suggested and encouraged this work. The hospitality of the Niels Bohr Institute is also appreciated.

References

1) H. Morinaga, Phys. Rev. **101** (1956) 254
2) D. M. Brink and G. F. Nash, Nuclear Physics **40** (1963) 608

3) G. E. Brown and A. M. Green, Nuclear Physics **75** (1966) 401
4) J. Borysowicz and R. Sheline, Phys. Lett. **12** (1964) 219
5) D. Brink and G. Bertsch, and E. Boeker, unpublished
6) T. Engeland, Nuclear Physics **72** (1965) 68
7) G. E. Brown, Congres International de Physique Nucleaire, Vol. 1, Paris (1964) p. 129
8) P. Federmand and I. Talmi, Phys. Lett. **15** (1965) 165
9) J. P. Elliot, Proc. Roy. Soc. **A245** (1958) 562
10) J. P. Elliot and M. Harvey, Proc. Roy. Soc. **A272** (1963) 557
11) S. G. Nilsson, Mat. Fys. Medd. Dan. Vid. Selsk. **29**, No. 16 (1955)
12) L. Zamick, Phys. Lett. **20** (1966) 176
13) G. Bertsch, Nuclear Physics **79** (1966) 209
14) A. Arima and S. Yoshida, Nuclear Physics **12** (1959) 139
15) J. D. McCullen, B. F. Bayman and L. Zamick, Phys. Rev. **134** (1964) B515
16) P. Federman, Phys. Lett. **20** (1966) 174
17) I. Kelson and C. A. Levinson, Phys. Rev. **134** (1964) B269
18) R. D. Lawson, Phys. Rev. **124** (1961) 1500
19) A. Kallio and K. Kolltveit, Nuclear Physics **53** (1963) 87
20) R. K. Bhaduri and E. L. Tomusiak, Proc. Phys. Soc. **86** (1965) 451
21) A. Kallio, Phys. Lett. **18** (1965) 51
22) R. W. Bauer *et al.*, Phys. Lett. **14** (1965) 129
23) L. L. Lee, J. P. Schiffer and D. Gemmell, Phys. Rev. Lett. **10** (1963) 496
24) J. W. Nelson, J. D. Oberholtzer and H. S. Plendl, Nuclear Physics **62** (1965) 434
25) B. M. Hinds and R. Middleton, to be published
26) A. Bohr and B. Mottelson, Mat. Fys. Medd. Dan. Vid. Selsk. **26**, No. 14 (1952)
27) S. Fallieros and R. A. Ferrell, Phys. Rev. **116** (1959) 660
28) G. Bertsch, Phys. Lett. **21** (1966) 70
29) D. Blum, P. Barreau and J. Bellicard, Phys. Lett. **4** (1963) 109
30) D. Youngblood, J. Aldridge and C. Class, Phys. Lett. **18** (1965) 291
31) R. Kloepper, R. Day and D. Lind, Phys. Rev. **114** (1959) 240
32) F. R. Metzger and G. K. Tandon, to be published
33) P. C. Simms, N. Benczer-Koller and C. S. Wu, Phys. Rev. **121** (1961) 1169
34) N. Benczer-Koller, M. Nessin and T. Kruse, Phys. Rev. **123** (1961) 262
35) C. Noack, Phys. Lett. **5** (1963) 276
36) B. Bayman, A. Reiner and R. Sheline, Phys. Rev. **115** (1959) 1627
37) C. Glashausser, M. Kondo, M. E. Rickey and E. Rost, Phys. Lett. **14** (1965) 113
38) R. Bock, H. H. Duhm and R. Stock, Phys. Lett. **18** (1965) 61
39) A. de-Shalit, Phys. Rev. **122** (1961) 1530
40) A. Bohr and B. Mottelson, 1962 lectures on nuclear structure and energy spectra
41) R. Middleton and D. J. Pullen, Nuclear Physics **51** (1964) 63
42) J. H. Bjerregaard *et al.*, Phys. Rev. **136** (1964) B1348
43) J. McCullen and R. Haight, private communication
44) B. Bayman, unpublished
45) G. Mitchell, private communication
46) C. Whitten, private communication